

Prediction of gas leakage and dispersion in utility tunnels based on CFD-EnKF coupling model

A 3D full-scale application

Cai, Jitao; Wu, Jiansong; Yuan, Shuaiqi; Kong, Desheng; Zhang, Xiaole

DOI

[10.1016/j.scs.2022.103789](https://doi.org/10.1016/j.scs.2022.103789)

Publication date

2022

Document Version

Accepted author manuscript

Published in

Sustainable Cities and Society

Citation (APA)

Cai, J., Wu, J., Yuan, S., Kong, D., & Zhang, X. (2022). Prediction of gas leakage and dispersion in utility tunnels based on CFD-EnKF coupling model: A 3D full-scale application. *Sustainable Cities and Society*, 80, Article 103789. <https://doi.org/10.1016/j.scs.2022.103789>

Important note

To cite this publication, please use the final published version (if applicable). Please check the document version above.

Copyright

Other than for strictly personal use, it is not permitted to download, forward or distribute the text or part of it, without the consent of the author(s) and/or copyright holder(s), unless the work is under an open content license such as Creative Commons.

Takedown policy

Please contact us and provide details if you believe this document breaches copyrights. We will remove access to the work immediately and investigate your claim.

Prediction of gas leakage and dispersion in utility tunnels based on CFD-EnKF coupling model: a 3D full-scale application

Abstract: Natural gas compartment accommodated in utility tunnels is beneficial in meeting the pressing demand of energy supply and sustainable urban environment. However, the leaking gas characterized by flammable and explosive can pose a huge threat to the safe operation of the utility tunnel. When an unexpected gas leakage accident happens in the actual situation, the prior information associated with the leakage source is commonly unclear or unknown. Therefore, the absence of an available tool for reasonable leakage and dispersion prediction in the above scenario precludes the timely and appropriate emergency response treatment. In this study, a three-dimensional source term estimation (3D-STE) model with the combination of the computational fluid dynamics (CFD) and ensemble Kalman filter (EnKF) algorithm is proposed to achieve spatiotemporal gas concentration prediction and gas emission source estimation. In the proposed approach, the observation data can be incorporated into the gas dispersion simulations continuously, thus the simulation results can be revised by the observation data and the source term estimation of gas leakage can be achieved by employing the EnKF algorithm. A twin experiment is employed to validate the effectiveness and practicability of the proposed model. The results show that the

1 proposed model can revise the prior errors in the gas leakage rate significantly and
2
3
4 obtain an accurate prediction of gas concentration distribution as well as gas leakage
5
6
7 rate. A feasible framework is also proposed serving as a good paradigm for the 3D-STE
8
9
10 model application. This study helps for consequence assessment and emergency
11
12
13 response of gas leakage accidents in utility tunnels.
14
15
16

17 **Keywords**

18
19 Utility tunnel; Gas leakage; Computational fluid dynamics; Ensemble Kalman
20
21
22 filter; OpenFOAM
23
24
25
26

27 **1. Introduction**

28
29
30
31
32
33 With the worldwide trend of rapid urbanization, there are increased demands for
34
35
36 sustainable cities development (Broere, 2016; Marzouk and Othman, 2020). The
37
38
39 construction of utility tunnels leads to an upsurge of interest because it shows a great
40
41
42 advantage in the clean energy supply and urban planning (Wang et al., 2018; Yang et
43
44
45 al., 2019; Yin et al., 2020). However, many types of municipal pipelines (e.g., gas
46
47
48 pipelines, sewage pipelines, heating pipelines, and water supply pipelines) are housed
49
50
51 in utility tunnels, which causes a spatial concentration of multiple hazards (Bai et al.,
52
53
54
55
56
57
58
59
60
61
62
63
64
65

1 explosion, and other cascading accidents. Meanwhile, the leakage of natural gas is also
2
3
4 an environmental concern since methane is an extremely environment-harmful
5
6
7 greenhouse gas that can speed up global warming (Cai et al., 2021). Therefore, gas
8
9
10 leakage in utility tunnels can cause unexpected and severe consequences in the context
11
12
13 of casualties, economic losses, and environmental problems, which should be given
14
15
16 sufficient attention from the perspective of consequence assessment and emergency
17
18
19 response.
20
21
22
23

24 Natural gas pipeline leakage in utility tunnel scenarios was mainly investigated
25
26
27 by previous studies through CFD simulations as well as some reduced-scale
28
29
30 experiments. Wang et al. (2020) first employed a two-dimensional numerical model to
31
32
33 investigate the effect of leakage size, pipeline pressure, and mechanical ventilation on
34
35
36 gas dispersion in utility tunnels. However, the complex environment in utility tunnels
37
38
39 caused by mechanical ventilation and the obstruction from facilities brings huge
40
41
42 difficulties to gas dispersion simulation. Such tricky situations may not be well resolved
43
44
45 by a simplified two-dimensional model (Lu et al., 2018; Li et al., 2019). Therefore, the
46
47
48 three-dimensional numerical model for simulating the gas leakage accidents in utility
49
50
51 tunnel scenarios has attracted more and more attention in recent years (Tan et al., 2017;
52
53
54 Lu et al., 2018; Li et al., 2019; Zhang et al., 2020; Zhou et al., 2021; Bu et al., 2021).
55
56
57
58
59
60
61
62
63
64
65

1 Tan et al. (2017) compared dispersion characteristics of two kinds of gravity gases
2
3
4 considering whether there is an available ventilation mode. The results indicated that
5
6
7 ventilation can disrupt the concentration stratification and reduce gas accumulation. Liu
8
9
10 et al. (2019) employed the realizable k-epsilon model to study the gas diffusion taking
11
12
13 into account ambient temperature and humidity. It revealed that the kinetic energy of
14
15
16 methane molecular motion was proportional to temperature, which subsequently caused
17
18
19 a larger diffusion coefficient and more rapid spread of natural gas. Zhang et al. (2020)
20
21
22 investigated the effect of ventilation velocities and sizes on the gas dispersion behaviors
23
24
25 in the utility tunnels. Meanwhile, the optimal ventilation configurations were proposed
26
27
28 from the aspect of economy, efficiency, and safety. Zhou et al. (2021; 2022) built a
29
30
31 utility tunnel mockup and the accuracy of the random opening air supply model and
32
33
34 standard k-epsilon turbulence model was confirmed through numerical and
35
36
37 experimental comparison. Moreover, gas monitoring sensor networks are optimized
38
39
40 through the CFD-adjoint-based method. Bu et al. (2021) conducted a multi-factor
41
42
43 analysis to study the gas dispersion characteristics in utility tunnels. The methane
44
45
46 invasion distance (MID) equation was also concluded, which helps to provide a
47
48
49 reference for the installation of gas alarm devices. Except for investigating the gas
50
51
52 dispersion process influenced by multiple factors, Lu et al. (2018) presented a
53
54
55
56
57
58
59
60
61
62
63
64
65

1 numerical analysis with an emphasis on rush repairs, such as optimizing the
2
3
4 configurations of block valves and ventilation fans. As shown in the above studies, the
5
6
7 CFD simulations have great advantages in evaluating the consequence of specific gas
8
9
10 leakage scenarios without initial parameters uncertainty. However, there are still
11
12
13 varying degrees of errors in the prediction of gas leakage and dispersion by using CFD
14
15
16 techniques when an unexpected leakage accident occurs in the actual situation. These
17
18
19 errors primarily stem from the lack of source term information and wind field
20
21
22 perturbation induced by mechanical ventilation and complex facility layouts. Such an
23
24
25 ill-posed problem can deviate the simulation results from actual situations significantly,
26
27
28 which prohibits real-time consequence assessment and reasonable emergency response
29
30
31 treatment.
32
33
34
35
36
37

38 Source term estimation (STE) methods are developed to identify the unknown
39
40
41 source information based on limited and noisy observation data, which has great
42
43
44 potentials in leakage source estimation and error suppression. As the two most attractive
45
46
47 and dominant approaches of STE methods (Xue et al., 2018; Wu et al., 2020), many
48
49
50 optimization-based and probabilistic-based methods have been used to accomplish the
51
52
53 inverse problem of gas dispersion, such as the ensemble Kalman filter method (Zhang
54
55
56 et al., 2015a; Zhang et al., 2015b; Zhang and Huang, 2017; Wang et al., 2019; Wu et
57
58
59
60
61
62
63
64
65

1 al., 2021) and Bayesian inference method (Wang et al., 2017; Xue et al., 2017; Xue et
2
3
4 al., 2018). Moreover, data-driven methods were also adopted to achieve source term
5
6
7 estimation with the rapid development of machine learning and deep learning (Ma and
8
9
10 Zhang, 2016; Kim et al., 2019; Ma et al., 2021). However, the current researches
11
12 associated with source term estimation are mainly restricted to atmospheric
13
14 environment scenarios. Utility tunnels characterized by confined and ventilated space
15
16
17 poses great difficulties for source term estimation and accurate gas dispersion
18
19
20 prediction, which needs to be further investigated. Yuan et al. (2019) and Wu et al.
21
22
23
24
25
26
27 (2020) have proposed an EnKF-based model and Bayesian inference-based model
28
29
30 respectively for predicting the gas dispersion process and reconstructing the leakage
31
32
33 source in utility tunnels. However, the gas transport process is determined on the basis
34
35
36
37 of the one-dimensional advection-diffusion equation, which has significant difficulties
38
39
40
41 in handling the three-dimensional facilities layout, turbulent diffusion, and gravity-
42
43
44 driven multicomponent transportation. Therefore, the further endeavor could be the
45
46
47 development of the high confidence three-dimensional gas dispersion model and
48
49
50 combining it with the source term estimation method. This can help to reproduce a more
51
52
53 realistic gas dispersion scenario as well as the estimation of the leakage source.
54
55
56
57 Moreover, dynamic ventilation conditions adopted in the operation of utility tunnels in
58
59
60

1 real leakage situations have not been fully considered. This may lead to some
2
3
4 inaccuracy in the prediction of gas leakage and dispersion process, which represents a
5
6
7 practical issue that needs to be addressed.
8
9

10
11 In this study, a three-dimensional source term estimation model is proposed to
12
13 improve the prediction accuracy of gas leakage and dispersion in utility tunnels. Firstly,
14
15 the three-dimensional CFD-based gas dispersion model is developed based on the
16
17 OpenFOAM platform and validated by experimental data. Then, the 3D-STE model
18
19 can be built by combining the gas dispersion model and the EnKF algorithm.
20
21 Furthermore, a twin experiment is employed to validate the proposed model
22
23 considering the dynamic ventilation condition of utility tunnels. The effectiveness of
24
25 the proposed model is evaluated qualitatively and quantitatively in the twin experiment
26
27 in terms of gas concentration distribution and source term (leakage velocity) estimation.
28
29 This study can provide effective technical supports for safety control and emergency
30
31 response of gas leakage accidents in utility tunnels.
32
33
34
35
36
37
38
39
40
41
42
43
44
45
46

47 **2. Methodology**

48
49 The proposed 3D-STE model consists of the CFD-based gas dispersion model and
50
51 the EnKF algorithm. In this section, the basic equations related to the gas dispersion
52
53 model and the EnKF algorithm are introduced respectively. Furthermore, the specific
54
55
56
57
58
59
60
61
62
63
64
65

1 procedure for conducting the proposed model is elaborated.

2.1 Governing equation of CFD model

2
3
4
5
6
7
8 In this study, a three-dimensional compressible CFD solver based on the
9
10 OpenFOAM platform is developed for the simulation of gas leakage and dispersion in
11
12 the utility tunnel (Mack and Spruijt, 2013; Fiates and Vianna, 2016; Wu et al., 2021).
13
14
15 The OpenFOAM platform allows the integration of the EnKF algorithm and the gas
16
17 dispersion simulation expediently due to its high extensibility. The governing equations
18
19 adopted from OpenFOAM are presented as follows:
20
21
22
23
24
25
26

27 (i) Continuity equation

$$\frac{\partial \rho}{\partial t} + \nabla \cdot (\rho \mathbf{u}) = 0 \quad (1)$$

28 (ii) Momentum equation

$$\frac{\partial(\rho u)}{\partial t} + \nabla \cdot (\rho u \mathbf{u}) = -\frac{\partial p}{\partial x} + \nabla \cdot (\mu \nabla u) + F_x \quad (2)$$

$$\frac{\partial(\rho v)}{\partial t} + \nabla \cdot (\rho v \mathbf{u}) = -\frac{\partial p}{\partial y} + \nabla \cdot (\mu \nabla v) + F_y \quad (3)$$

$$\frac{\partial(\rho w)}{\partial t} + \nabla \cdot (\rho w \mathbf{u}) = -\frac{\partial p}{\partial z} + \nabla \cdot (\mu \nabla w) + F_z \quad (4)$$

29 (iii) Energy equation

$$\frac{\partial(\rho i)}{\partial t} + \nabla \cdot (\rho i \mathbf{u}) = -p \nabla \cdot \mathbf{u} + \nabla \cdot (k \nabla T) + \Phi + S_h \quad (5)$$

30 (iv) Multi-component transport equation

$$\frac{\partial}{\partial t} (\rho C_i) + \nabla \cdot (\rho C_i \mathbf{u}) = \nabla \cdot (D \nabla C_i) + S_i \quad (6)$$

1 (v) Gas state equation
2
3

$$4 \quad pV = nZRT \quad (7)$$

5
6
7 Where ρ is the mixed gas density, \mathbf{u} is the gas velocity vector. p is the pressure, μ
8 is the viscosity, F_x , F_y and F_z are the momentum source term in three directions. i
9
10 and T are internal thermal energy and temperature respectively. k is the thermal
11 conductivity coefficient, S_h is the internal heat source, and Φ is the dissipation
12 function. C_i represents the gas volume fraction of every species, D is diffusion
13 capacity coefficient and S_i is mass source term. V , n , Z , R are gas volume, amount
14 of substance, compressibility, and the gas constant respectively.
15
16
17
18
19
20
21
22
23
24
25
26
27
28
29
30

31 As a robust two-equation eddy-viscosity turbulence model, the shear stress
32 transport (SST) turbulence model was employed to simulate the turbulent flow
33
34
35
36
37
38 (Sklavounos and Rigas, 2004). And the corresponding equations are listed:
39

$$40 \quad \frac{\partial(\rho k)}{\partial t} + \nabla \cdot (\rho k \mathbf{u}) = \nabla \cdot ((\mu + \sigma_k \mu_t) \nabla k) + P - \rho \beta^* \omega k \quad (8)$$

$$41 \quad \frac{\partial(\rho \omega)}{\partial t} + \nabla \cdot (\rho \omega \mathbf{u}) = \nabla \cdot ((\mu + \sigma_\omega \mu_t) \nabla \omega) + \frac{\gamma}{v_t} P - \rho \beta \omega^2$$
$$42 \quad + 2(1 - F_1) \frac{\rho \sigma_\omega \omega^2}{\omega} \nabla k \nabla \omega \quad (9)$$

43
44
45
46
47
48
49
50
51 Where k and ω represent turbulence kinetic energy and turbulence dissipation rate.
52
53
54
55
56
57
58
59
60
61
62
63
64
65
66
67
68
69
70
71
72
73
74
75
76
77
78
79
80
81
82
83
84
85
86
87
88
89
90
91
92
93
94
95
96
97
98
99
100
101
102
103
104
105
106
107
108
109
110
111
112
113
114
115
116
117
118
119
120
121
122
123
124
125
126
127
128
129
130
131
132
133
134
135
136
137
138
139
140
141
142
143
144
145
146
147
148
149
150
151
152
153
154
155
156
157
158
159
160
161
162
163
164
165
166
167
168
169
170
171
172
173
174
175
176
177
178
179
180
181
182
183
184
185
186
187
188
189
190
191
192
193
194
195
196
197
198
199
200
201
202
203
204
205
206
207
208
209
210
211
212
213
214
215
216
217
218
219
220
221
222
223
224
225
226
227
228
229
230
231
232
233
234
235
236
237
238
239
240
241
242
243
244
245
246
247
248
249
250
251
252
253
254
255
256
257
258
259
260
261
262
263
264
265
266
267
268
269
270
271
272
273
274
275
276
277
278
279
280
281
282
283
284
285
286
287
288
289
290
291
292
293
294
295
296
297
298
299
300
301
302
303
304
305
306
307
308
309
310
311
312
313
314
315
316
317
318
319
320
321
322
323
324
325
326
327
328
329
330
331
332
333
334
335
336
337
338
339
340
341
342
343
344
345
346
347
348
349
350
351
352
353
354
355
356
357
358
359
360
361
362
363
364
365
366
367
368
369
370
371
372
373
374
375
376
377
378
379
380
381
382
383
384
385
386
387
388
389
390
391
392
393
394
395
396
397
398
399
400
401
402
403
404
405
406
407
408
409
410
411
412
413
414
415
416
417
418
419
420
421
422
423
424
425
426
427
428
429
430
431
432
433
434
435
436
437
438
439
440
441
442
443
444
445
446
447
448
449
450
451
452
453
454
455
456
457
458
459
460
461
462
463
464
465
466
467
468
469
470
471
472
473
474
475
476
477
478
479
480
481
482
483
484
485
486
487
488
489
490
491
492
493
494
495
496
497
498
499
500
501
502
503
504
505
506
507
508
509
510
511
512
513
514
515
516
517
518
519
520
521
522
523
524
525
526
527
528
529
530
531
532
533
534
535
536
537
538
539
540
541
542
543
544
545
546
547
548
549
550
551
552
553
554
555
556
557
558
559
560
561
562
563
564
565
566
567
568
569
570
571
572
573
574
575
576
577
578
579
580
581
582
583
584
585
586
587
588
589
590
591
592
593
594
595
596
597
598
599
600
601
602
603
604
605
606
607
608
609
610
611
612
613
614
615
616
617
618
619
620
621
622
623
624
625
626
627
628
629
630
631
632
633
634
635
636
637
638
639
640
641
642
643
644
645
646
647
648
649
650
651
652
653
654
655
656
657
658
659
660
661
662
663
664
665
666
667
668
669
670
671
672
673
674
675
676
677
678
679
680
681
682
683
684
685
686
687
688
689
690
691
692
693
694
695
696
697
698
699
700
701
702
703
704
705
706
707
708
709
710
711
712
713
714
715
716
717
718
719
720
721
722
723
724
725
726
727
728
729
730
731
732
733
734
735
736
737
738
739
740
741
742
743
744
745
746
747
748
749
750
751
752
753
754
755
756
757
758
759
760
761
762
763
764
765
766
767
768
769
770
771
772
773
774
775
776
777
778
779
780
781
782
783
784
785
786
787
788
789
790
791
792
793
794
795
796
797
798
799
800
801
802
803
804
805
806
807
808
809
810
811
812
813
814
815
816
817
818
819
820
821
822
823
824
825
826
827
828
829
830
831
832
833
834
835
836
837
838
839
840
841
842
843
844
845
846
847
848
849
850
851
852
853
854
855
856
857
858
859
860
861
862
863
864
865
866
867
868
869
870
871
872
873
874
875
876
877
878
879
880
881
882
883
884
885
886
887
888
889
890
891
892
893
894
895
896
897
898
899
900
901
902
903
904
905
906
907
908
909
910
911
912
913
914
915
916
917
918
919
920
921
922
923
924
925
926
927
928
929
930
931
932
933
934
935
936
937
938
939
940
941
942
943
944
945
946
947
948
949
950
951
952
953
954
955
956
957
958
959
960
961
962
963
964
965
966
967
968
969
970
971
972
973
974
975
976
977
978
979
980
981
982
983
984
985
986
987
988
989
990
991
992
993
994
995
996
997
998
999
1000

1 k-omega model is utilized in the region close to the boundary layer and switches to the
2
3
4 k-epsilon model in the vicinity of the free shear flow. The detailed description and
5
6
7 specific values of model parameters are summarized in Menter's study (Menter et al.,
8
9
10
11 2003).

14 2.2 Ensemble Kalman filter algorithm

17 Due to the implicit assumption of linear Gaussian state-space, the Ensemble
18
19
20
21 Kalman filter algorithm has a great advantage in avoiding the degeneracy problem of
22
23
24 reweighting-based data assimilation algorithms (Katzfuss et al., 2016). It promotes the
25
26
27 wide application of the EnKF algorithm in various scenarios because of its remarkable
28
29
30 robustness, such as river pollution scenarios (Zhang and Huang, 2017; Wang et al.,
31
32
33 2019), nuclear disasters scenarios (Zhang et al., 2015a; Zhang et al., 2015b), indoor
34
35
36 pollution scenario (Lin and Wang, 2013; Sharma et al., 2019), chemical plant scenario
37
38
39
40
41 (Wu et al., 2021), and confined space scenarios (Wu et al., 2018; Ji et al., 2018; Yuan
42
43
44 et al., 2019).

46
47 In this section, the basic equations of the EnKF algorithm are presented as follows:

48
49
50
51 (i) Forecast step:

$$52 X_t^f = M(X_{t-1}^f), X_t^f \in R^{n*N} \quad (10)$$

53
54
55
56
57
58 (ii) Analysis step:

$$X_t^a = X_{t-1}^f + K(Y_t^* - H * X_t^f) \quad (11)$$

Where Eq. (10) and Eq. (11) represent the main procedure of the EnKF algorithm, X_t^f is the state matrix at time t , it usually has n rows and N columns, n and N represent the parameters of interest and ensemble sizes respectively, X_t^a is analytical value revised by observation data. The M stands for the nonlinear dynamic model propagating state matrix over time, and H is a nonlinear observation operator transforming the state matrix to the corresponding observation sites. K represents the Kalman gain.

The forecast error covariance matrix can be calculated by Eq. (12).

$$P = \frac{1}{N-1} (X_t^f - \overline{X_t^f})(X_t^f - \overline{X_t^f})^T \quad (12)$$

Where P is the forecast error covariance matrix, $\overline{X_t^f}$ can be obtained by multiplying an average factor 1_N with N rows and N columns and every factor in 1_N is $1/N$.

The Kalman gain K serves as a weighted factor between the gas dispersion CFD model prediction and observation data. It can be obtained by Eq. (13).

$$K = PH^T(HPH^T + R_e)^{-1} \quad (13)$$

Where R_e is the observation error covariance matrix and can be calculated as follows:

$$E^{obs} = (\varepsilon_1, \varepsilon_2, \varepsilon_3, \varepsilon_4 \dots \varepsilon_k) \quad (14)$$

$$R_e = E^{obs} * (E^{obs})^T \quad (15)$$

Where E^{obs} is the observation error vector and ε represents the perturbation added to observation data.

In this study, the state matrix consists of N ensembles, and every vector contains gas concentrations and leakage velocity:

$$X = (x_1, x_2, x_3 \dots x_N) \in R^{n*N} \quad (16)$$

$$x_N = (c_1, c_2, c_3 \dots c_m, u_1 \dots u_l)^T \in R^{n=i+l} \quad (17)$$

Where x is the state vector, c is the leaked gas concentration. and u means the leakage velocity at the leakage hole. Moreover, m represents the total grid number including concentration data, l is the number of data assimilation steps. u_1 represent the initial-guess leakage velocity, which should be prescribed by users. Then, a new leakage velocity will be updated and added in the state vector x once a data assimilation step is completed.

$$u_l^b = \sum_{i=1}^N u_{l-1}^a(i) / N \quad (18)$$

$$u_l^f(i) = u_l^b + \delta u_l^b(i) \quad (19)$$

Where $u_{l-1}^a(i)$ is the revised leakage velocity of the latest time step at corresponding ensemble i , the ensemble average leakage velocity u_l^b is used to generate the new leakage velocity ensemble for the next time step by adding noise $\delta u_l^b(i)$, which can be calculated by Eq. (20).

$$\delta u_l^b(i) = \alpha u_{l-1}^a(i) + \sqrt{1 - \alpha^2} r_{l-1}(i) \sigma \quad (20)$$

Where α represents the influence of the latest leakage velocity on the determination of the leakage velocity at the next time steps and is set as 0.99 in this study. $r_{l-1}(i)$ is a random number following Gaussian distribution $N \sim (0,1)$. And σ is the standard deviation of the latest leakage velocity ensemble u_{l-1}^a .

2.3 Three-dimensional STE model

With the combination of the CFD-based gas dispersion mode and EnKF algorithm, the three-dimension STE model can be developed. The EnKF algorithm allows integrating the observation data into the three-dimensional gas dispersion model and helps to suppress errors resulting from the numerical simulation and the observation sensors/sites. It helps to improve the prediction accuracy of the spatial-temporal distribution of leaked gas and further achieves a reasonable leakage source estimation in utility tunnels. The complex scenarios in utility tunnels are characterized by confined underground space equipped with various facilities and forced ventilation. Such complex scenarios bring huge difficulties to the inversion models. The inverse problems in utility tunnels have not been resolved well by previous studies in the aspect of both source term estimation and three-dimensional gas concentration prediction. The specific implementation of the three-dimensional STE model is presented in Fig. 1.

1 Generally, the leakage source term is unknown when an unexpected leakage
 2
 3
 4 accident happened in real situations. The leakage source distribution with inevitable
 5
 6
 7 prior errors should be initialed by users in the CFD model to conduct gas leakage and
 8
 9
 10
 11 dispersion simulations. The prior leakage source term and corresponding gas
 12
 13
 14 concentration distribution results will be revised by the EnKF algorithm whenever the
 15
 16
 17 observation data is available. Finally, the revised leakage source and gas concentration
 18
 19
 20
 21 distribution are utilized to reconstruct the revised state matrix for the next iteration. As
 22
 23
 24 the data assimilation process goes on, the revised predictions of gas concentration
 25
 26
 27
 28 distribution and gas leakage source term can be obtained.

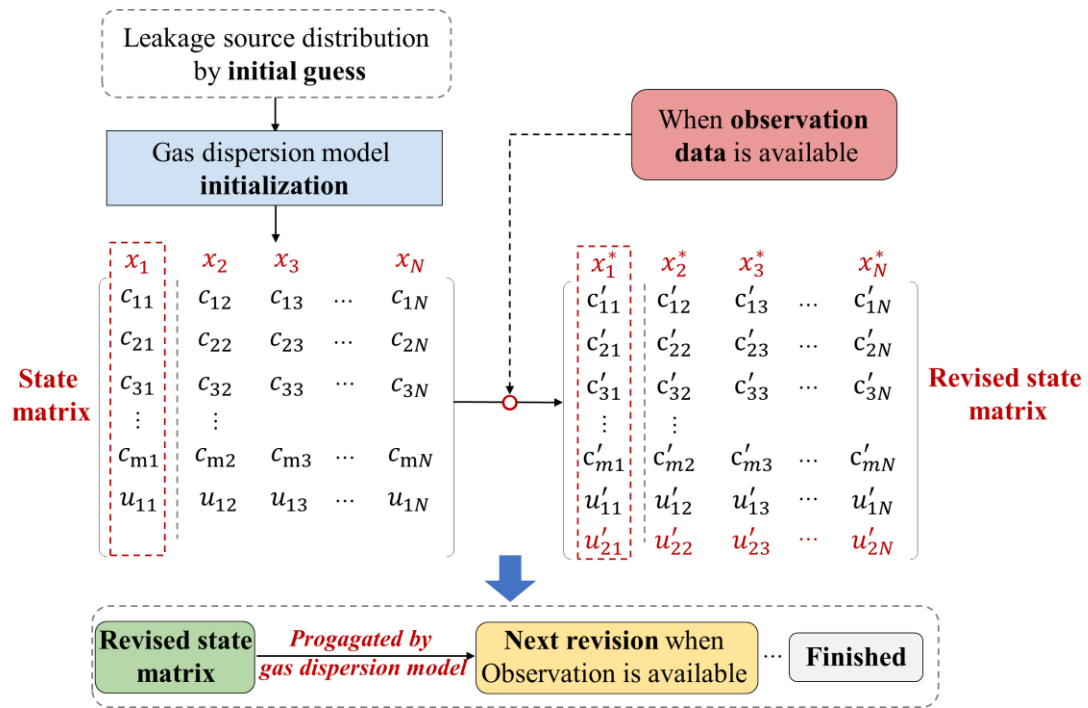


Fig. 1 Specific implementation of three-dimensional STE model.

3. Model validations

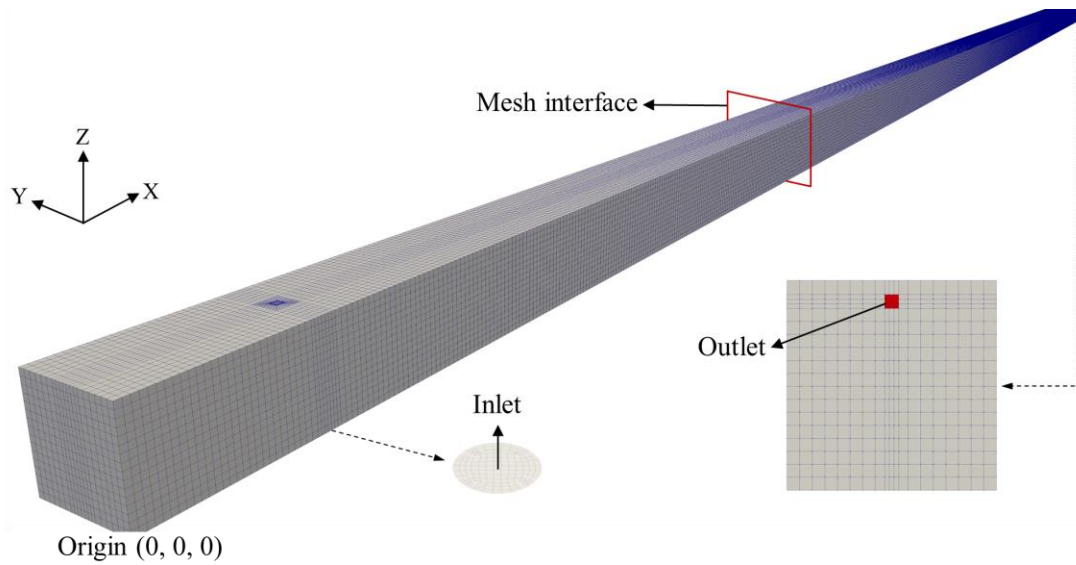
3.1 Validation of gas dispersion model

Generally, the unsatisfactory performance of the gas dispersion model will greatly weaken the accuracy of the estimation method (Ma et al., 2016; Ma et al., 2021). In order to illustrate the gas dispersion model can capture the detailed flow field when an accidental leakage occurs. It is common practice that the experimental data are used to be compared with the prediction results of the gas dispersion model. Most existing experiments, also numerical model validation, associated with gas leakage in the utility tunnel use alternative gases such as CO₂ and neon due to the potential fire/explosion risk by using methane (Bu et al., 2021; Zhou et al., 2020; Wang et al., 2020). Considering both the feasibility for model validation and the availability of the experiment data, the experimental data obtained from Fang et al. (2006) are employed to validate the feasibility and accuracy of the gas dispersion model.

3.1.1 Numerical configurations

In Fang's study, a reduced-scale utility tunnel system was designed to investigate the gas dispersion process in the confined space, and the quantitative comparison by using numerical simulation was also involved. The investigated utility tunnel has a dimension of 10 m × 0.15 m × 0.15 m, which is displayed in Fig. 2. A rectangular

1 window with a dimension of 0.01 m × 0.01 m was set as the gas vent. Carbon dioxide
 2
 3
 4 was utilized as an alternative gas to methane considering safety requirements. The CO₂
 5
 6
 7 gas was released from a circular hole with a diameter of 0.02 m. Meanwhile, a total of
 8
 9
 10
 11 49 gas sensors were employed to detect the CO₂ concentration along the centerline of
 12
 13
 14 the utility tunnel mode. The distance between two gas sensors is set as 0.2 m. The
 15
 16
 17 specific parameters related to this experiment are listed in Table 1.
 18
 19
 20
 21



22
 23
 24
 25
 26
 27
 28
 29
 30
 31
 32
 33
 34
 35
 36
 37
 38
 39
 40
 41
 42
 43
 44
 45
 46
 47
 48
 49
 50
 51
 52
 53
 54
 55
 56
 57
 58
 59
 60
 61
 62
 63
 64
 65

Fig. 2 Geometric and mesh schematic of the utility tunnel system.

Table 1 Specific configurations of the gas release experiment

Parameter	Value
Length of the utility tunnel system (m)	10
Width of the utility tunnel system (m)	0.15
Height of the utility tunnel system (m)	0.15
Location of leakage hole (m)	(0.28, 0, 0)
Location of the sampling centerline (m)	(0, 0.075, 0.075) to (10, 0.075, 0.075)
Location of NO.16 gas sensor (m)	(3.1, 0.075, 0.075)

Release flow rate (L/min)	4
Environmental temperature (K)	293
Total experiment time (s)	300

As shown in Fig. 2, the computational domain of the utility tunnel model is discretized by using a hexahedral cell scheme (Duan et al., 2015). To avoid the sharp aspect ratio of cells, the computational domain is divided into two sub-parts for hexahedral discretization. Such operation will cause a misaligned mesh interface but can be handled by the arbitrary mesh interface (AMI) technique (Carneiro et al., 2019).

By referring to the experimental configuration in Fang's study, the specific boundary conditions applied in this study are summarized as follows:

(i) Inlet: *flowRateInletVelocity* condition is employed to provide a stable volumetric flow rate, which is set as 4 L/min.

(ii) Outlet: *pressureInletOutletVelocity* condition is used to serve as a pressure outlet, and the pressure value is prescribed as 101325 Pa.

(iii) Mesh interface: *cyclicAMI* condition is introduced to handle the data exchange by interpolation calculation.

(iv) Walls: All the walls are defined as the *no-slip* condition.

3.1.2 Results analysis

Firstly, mesh independence analysis was conducted to ensure the mesh-

1 independent results. The CO₂ concentration along the sampling centerline (mentioned
2
3
4 in Table 1) at 120 s was utilized to evaluate the differences between four mesh schemes.
5
6
7 The comparison of the simulation results obtained by using four different mesh schemes
8
9
10 with grid numbers of 100 thousand, 200 thousand, 300 thousand, and 400 thousand is
11
12
13 presented in Fig. 3. As shown in Fig. 3, although the simulation results of four mesh
14
15
16 schemes have a similar tendency, Mesh_1 and Mesh_2 schemes have a relatively large
17
18 deviation in both CO₂ concentration and dispersion distance compared to the Mesh_3
19
20
21 deviation in both CO₂ concentration and dispersion distance compared to the Mesh_3
22
23
24 scheme. As the stepwise refinement of grids, there is a reasonable difference between
25
26
27 Mesh_3 and Mesh_4 schemes (the max relative error and average relative error are 8.79%
28
29
30 and 1.55% respectively). Therefore, Mesh_3 is considered suitable for the following
31
32
33
34
35 simulations and analysis with both acceptable accuracy and low computational load.
36
37

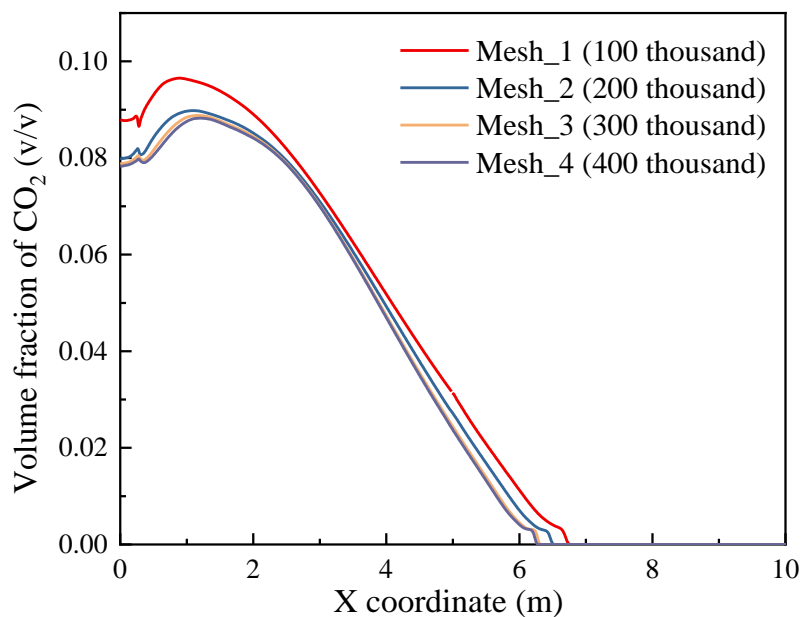


Fig. 3 Mesh independence analysis.

1 In order to validate the gas dispersion model quantitatively, CO₂ monitoring data
2
3
4 obtained from Fang et al. (2006) were adopted for further comparison. Fig. 4 presents
5
6
7 the CO₂ concentration comparison between simulation results and experimental data at
8
9
10 the location of the No.16 gas sensor (mentioned in Table 1). As shown in Fig. 4, There
11
12
13 is one relatively large deviation between simulation results and experimental data at 60
14
15
16 s with a 34 % relative error, which can be seen in Fang's study similarly. The reason for
17
18
19 this may be the uncontrollable error induced by measurement equipment and the
20
21
22 ambient environment. Overall, the simulation results of the gas dispersion model
23
24
25 achieved a reasonable agreement with the experimental data. Most of the relative errors
26
27
28 between the simulation results and experimental data are less than 10.00 %. And the
29
30
31 average relative errors between simulations and experimental data is 9.73 %. It
32
33
34 indicates that the gas dispersion model can well capture the dispersion behaviors of
35
36
37 gravity-driven gas flow in the confined space scenario (Wang et al., 2020; Zhang et al.,
38
39
40 2020). Therefore, it can be used for the prediction of gas leakage and dispersion in
41
42
43 utility tunnel scenarios with good accuracy.
44
45
46
47
48
49
50
51
52
53
54
55
56
57
58
59
60
61
62
63
64
65

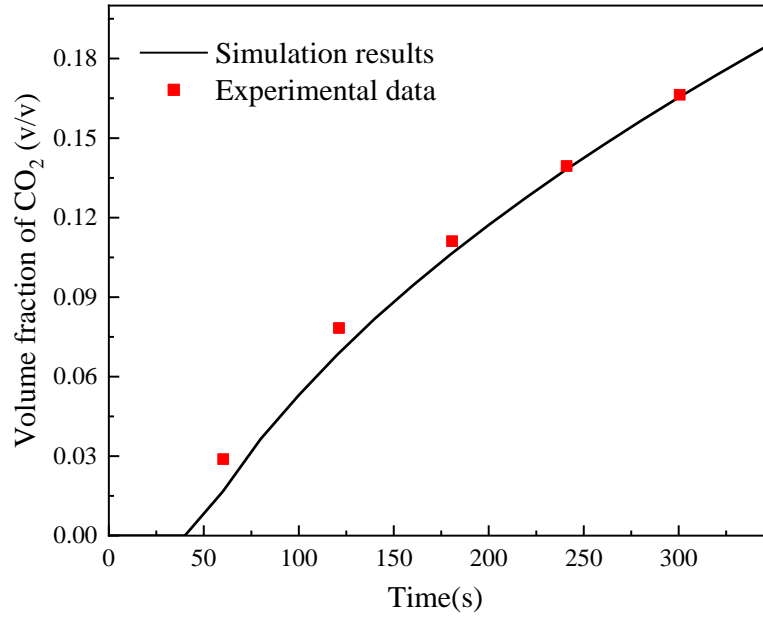


Fig. 4 CO₂ concentration comparison at the No.16 gas sensor.

3.2 3D-STE model validation

After the validation of the gas dispersion model, it can be integrated with the EnKF algorithm to achieve the gas dispersion prediction and leakage source estimation in the utility tunnel. A twin experiment, which was already been applied for evaluating the data assimilation models (Zhang et al., 2014; Yuan et al., 2019), was employed to validate the effectiveness and practicability of the proposed 3D-STE model.

3.2.1 Configurations

In this section, the computational domain is built and discretized by using the blockMesh and snappyHexMesh tools, which are involved in the OpenFOAM platform for the hexahedral mesh generation. The configuration of the computational domain was determined by referring to the underground utility tunnel of Changbin Road in

Haikou City. The geometric layout and boundary conditions of the computational domain are shown in Fig. 5. Moreover, Table 2 summarizes the configuration parameters related to the calculations.

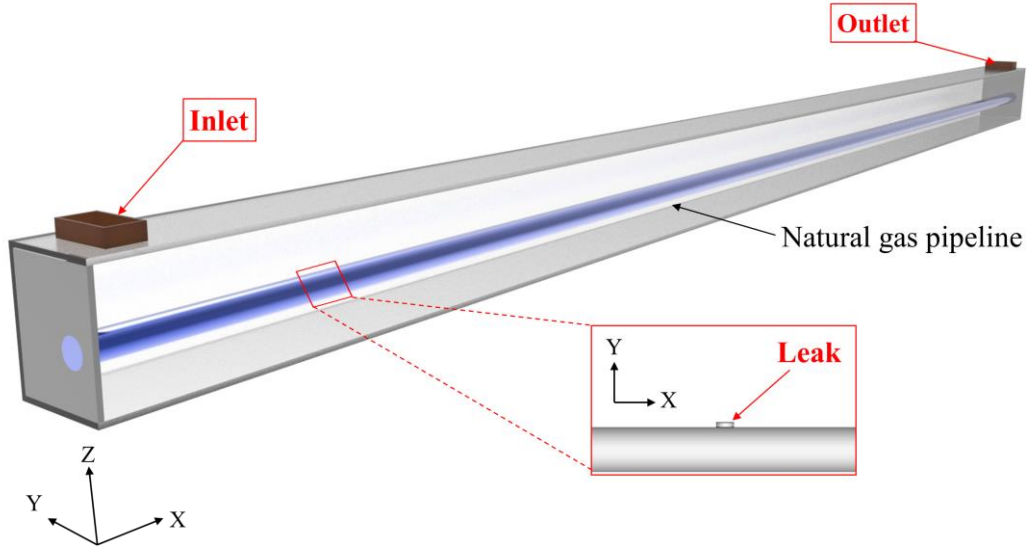


Fig. 5 Geometric and boundary conditions of the utility tunnel.

Table 2 Configuration parameters of the utility tunnel.

Parameter	Value
Length of the utility tunnel (m)	200
Width of the utility tunnel (m)	2
Height of the utility tunnel (m)	2.4
Location of leakage hole (m)	(45, 0.9, 0.6)
Diameter of leakage hole (mm)	100
Diameter of the gas pipeline (mm)	500
Normal air exchange frequency (h^{-1})	6
Accidental air exchange frequency (h^{-1})	12
Environmental temperature (K)	293

The determination of the adopted boundary conditions and the corresponding

1 parameter values is presented as follows:
2
3

4 (1) Inlet: The user-defined *codedFixedValue* condition is used to provide a time-
5
6
7 dependent ventilation condition considering the dynamic transformation of air
8
9
10 exchange frequency when an unexpected leakage accident occurs in the utility tunnel.
11

12
13
14 By referring to Eq. (21) (CPS, 2015), the ventilation velocities of the Inlet are set as 1.6
15
16
17 m/s and 3.2 m/s for normal ventilation and accidental ventilation scenarios respectively.
18
19

$$20 \quad v_{Inlet} = \frac{n \times V}{3600 \times F} \quad (21)$$

21
22
23
24 Where n is the air exchange frequency, F is the area of the ventilation vent, and V
25
26
27 represents the volume of the utility tunnel.
28
29

30
31 (2) Outlet: The *pressureInletOutletVelocity* condition is employed to define a
32
33
34 pressure outlet, and the pressure value is set as 101325 Pa.
35
36

37
38 (3) Leak: The *fixedValue* condition is selected to define a stable leakage velocity
39
40
41 and the leakage velocity of the leakage hole is set as 15 m/s.
42
43

44 (4) Walls: All the walls are defined as the *noSlip* condition.
45
46

47
48 Moreover, in order to model a more real leakage scenario, the steady flow field
49
50
51 without leakage is computed firstly to initialize the internal flow fields for the leakage
52
53
54 scenario.
55
56

57
58 The above-mentioned configuration parameters were utilized in the control group
59
60

1 of the twin experiment for representing an assumed real situation (using initial
2
3
4 parameters without uncertainty). In the data assimilation (DA) group of the twin
5
6
7 experiment, the initial-guess parameters are employed. Thus the effectiveness of the
8
9
10 3D-STE model can be validated by comparing the difference between the control group
11
12
13 and the DA group. In this study, the initial-guess leakage velocity ensemble is assumed
14
15
16 to follow a uniform distribution, which can be observed in Fig. 6. Meanwhile, a normal
17
18
19 distribution noise of $N\sim(0,0.1)$ is added to the airflow ensemble considering the
20
21
22 uncertainty resulting from ventilation perturbation in the confined space. Fig. 7 presents
23
24
25 84 observation sites in the control group. The corresponding collected observation data
26
27
28 will be utilized to revise the concentration distribution and reconstruct the gas leakage
29
30
31 rate of the DA group. And ensemble Inflation is used to modify the prior ensemble
32
33
34 estimates of the state matrix to reduce filter error and avoid filter divergence (Anderson,
35
36
37 2007). Finally, the detailed configuration parameters used in the three-dimensional STE
38
39
40
41 model are listed in Table 3.
42
43
44
45
46
47
48
49
50
51
52
53
54
55
56
57
58
59
60
61
62
63
64
65

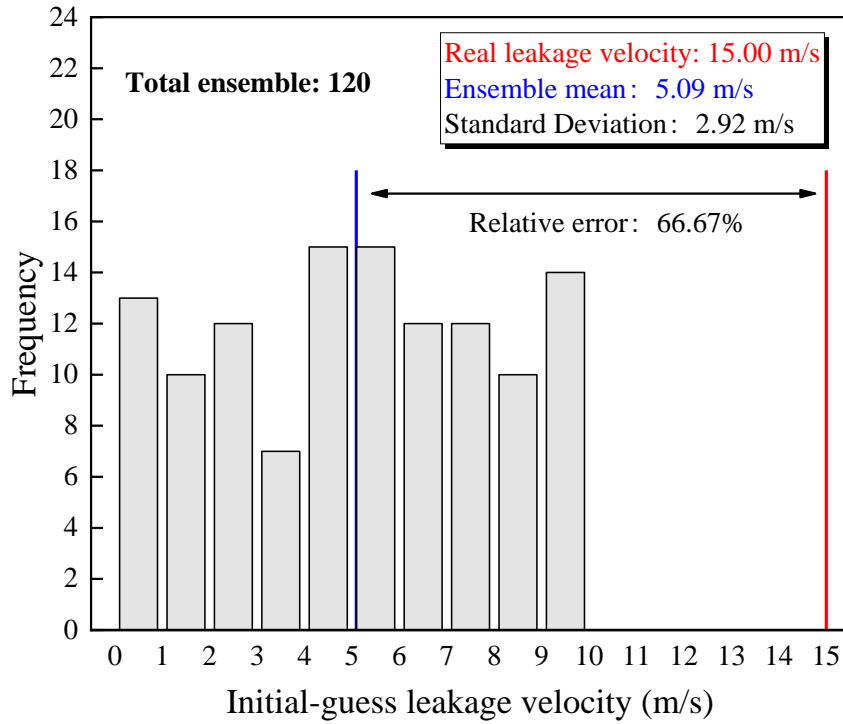


Fig. 6 Prior leakage velocity ensemble obtained by initial guess.

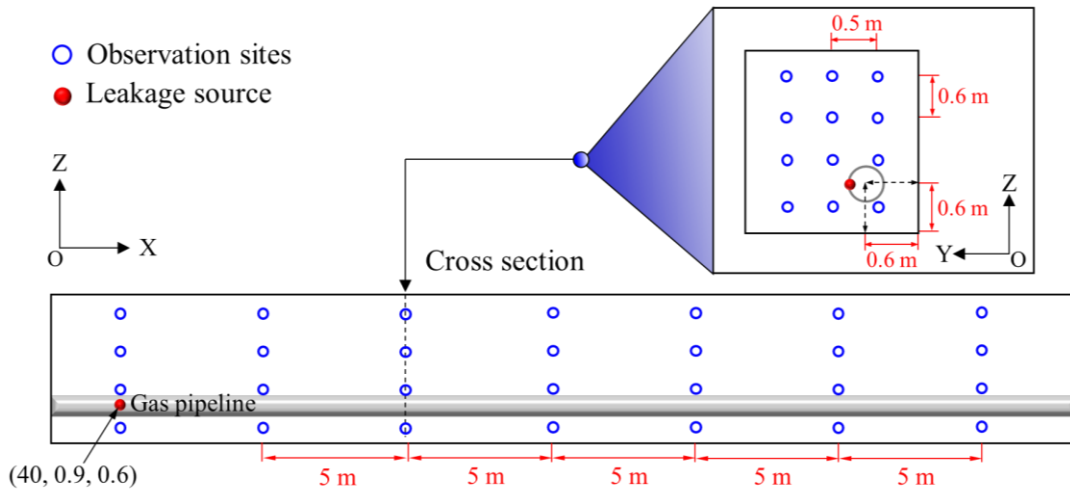


Fig. 7 Specific layout of the observation sites.

Table 3 Configuration parameters of the 3D-STE model.

Parameter	Value
Ensemble size	120
Ensemble inflation	1.0
Observation site number	84

Data assimilation frequency (s ⁻¹)	0.5
Total simulation time (s)	30
Total data assimilation steps	60

3.2.2 Prediction of gas spatiotemporal distribution

According to the regulation of GB50838-2015 *Technical Specification for Urban utility Tunnel Engineering*, the air exchange frequency will shift from 3 to 6 when the gas alarm threshold (1% VOL) is reached. This dynamic transformation of ventilation conditions can bring perturbation to the flow field, especially for the confined space with facilities. In this section, such dynamic and complex scenarios will be used to test the effectiveness of the proposed model with both qualitative and quantitative comparisons.

Fig. 8 and Fig. 9 present the horizontal (X=40 m cross-section) and vertical (Y=1 m cross-section) comparisons of gas concentration distributions obtained from the control group, DA group, and reference group. The reference group was present here for demonstrating prediction results without the DA revision (i.e., activating the gas dispersion model only by initial-guess leakage velocity and no observation data is integrated). The leakage velocity of the reference group is set as the mean of the initial-guess ensemble (5.09 m/s). Thus, the effectiveness of the proposed model can be observed directly by comparing the difference between the control group, DA group,

1 and reference group. As can be seen from Fig. 8, the gas concentration distribution
2
3
4 between the DA group and the reference group has no apparent difference at the initial
5
6
7 stage ($T=5s$). There are two major reasons for this: (i) Although the prediction of the
8
9
10 DA group is calculated by the mean of ensembles, there is a great similarity existing
11
12
13 between the prior ensemble mean of the DA group and the leakage velocity of the
14
15
16 reference group; (ii) At the initial stage of natural gas leakage, the DA algorithm can
17
18
19 achieve negligible revision due to the limited observation data available. As time goes
20
21
22 on, a phenomenon can be observed that the released gas was diluted rapidly in the
23
24
25 reference group, which indicates a large deviation compared to the control group. This
26
27
28 is because the reference group cannot be revised by the DA algorithm and the relatively
29
30
31 low leakage velocity persist. Therefore, the gas concentration distribution shows a large
32
33
34 difference between the reference group and the control group under the effect of
35
36
37 dynamic ventilation. However, the gas concentration distribution of the DA group
38
39
40 shows a comparable prediction compared to the control group. This is because the
41
42
43 available observation data increased gradually, which were used to correct prior errors
44
45
46 in the DA group and finally achieved a more accurate prediction of the gas
47
48
49 concentration distribution. Similarly, the vertical concentration distribution of the DA
50
51
52 group becomes more comparable to the real concentration distribution in the control
53
54
55
56
57
58
59
60
61
62
63
64
65

1 group, which can be observed in Fig. 9. However, a difference still exists between the
2
3
4 control group and the reference group because the prior errors in the leakage source
5
6
7 term and cannot be revised by data assimilation. Meanwhile, it can be seen that the data
8
9
10 assimilation process in the horizontal and vertical sections is quite different in terms of
11
12
13 time series. The reason for this may be that the vertical section is relatively small and
14
15
16 narrow, in which the relatively steady condition can be achieved in a short time under
17
18
19 the effect of dynamic ventilation. Overall, the 3D-STE model can realize the reasonable
20
21
22 correction of the three-dimensional gas concentration distribution by assimilating
23
24
25
26
27 observation data into the gas dispersion model.
28
29
30
31
32
33
34
35
36
37
38
39
40
41
42
43
44
45
46
47
48
49
50
51
52
53
54
55
56
57
58
59
60
61
62
63
64
65

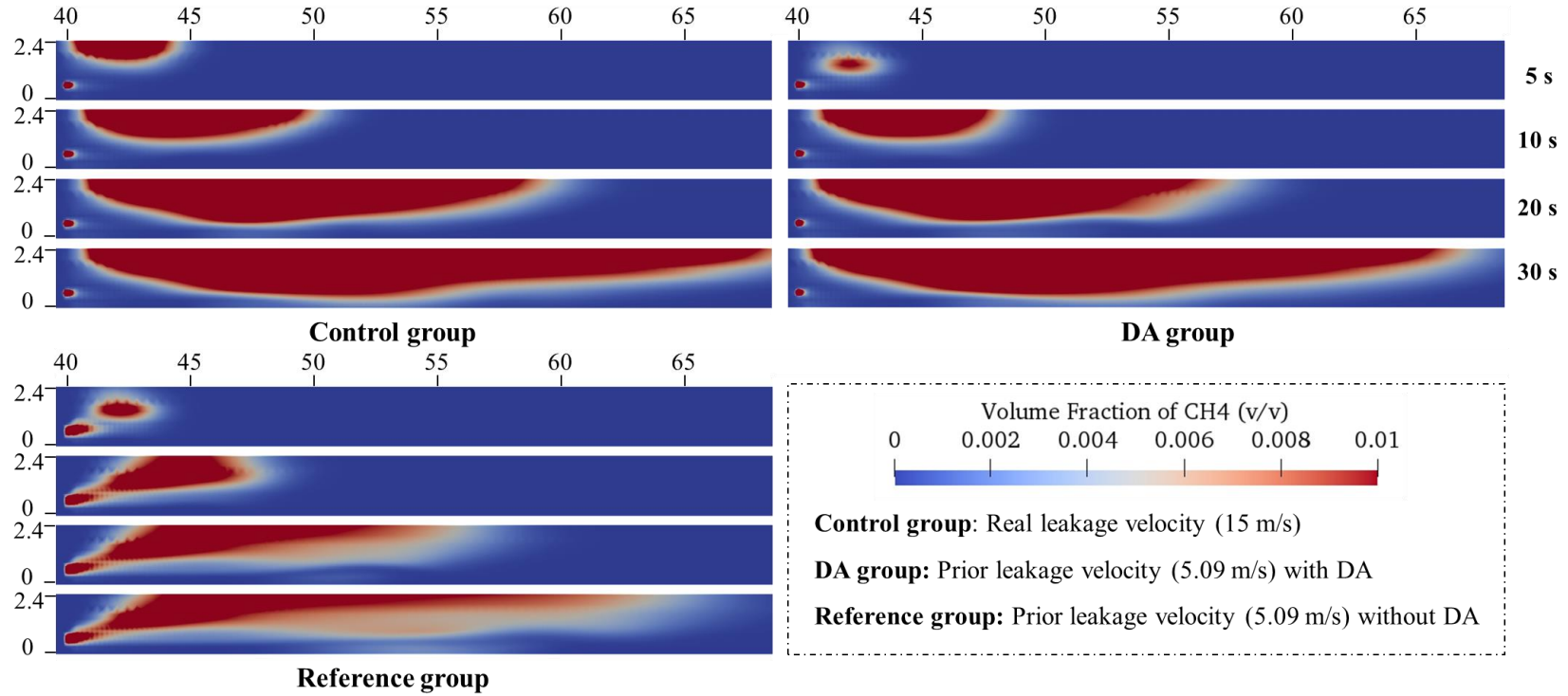


Fig. 8 Comparison between the control group, the DA group, and the reference group at Y=1 m cross-section.

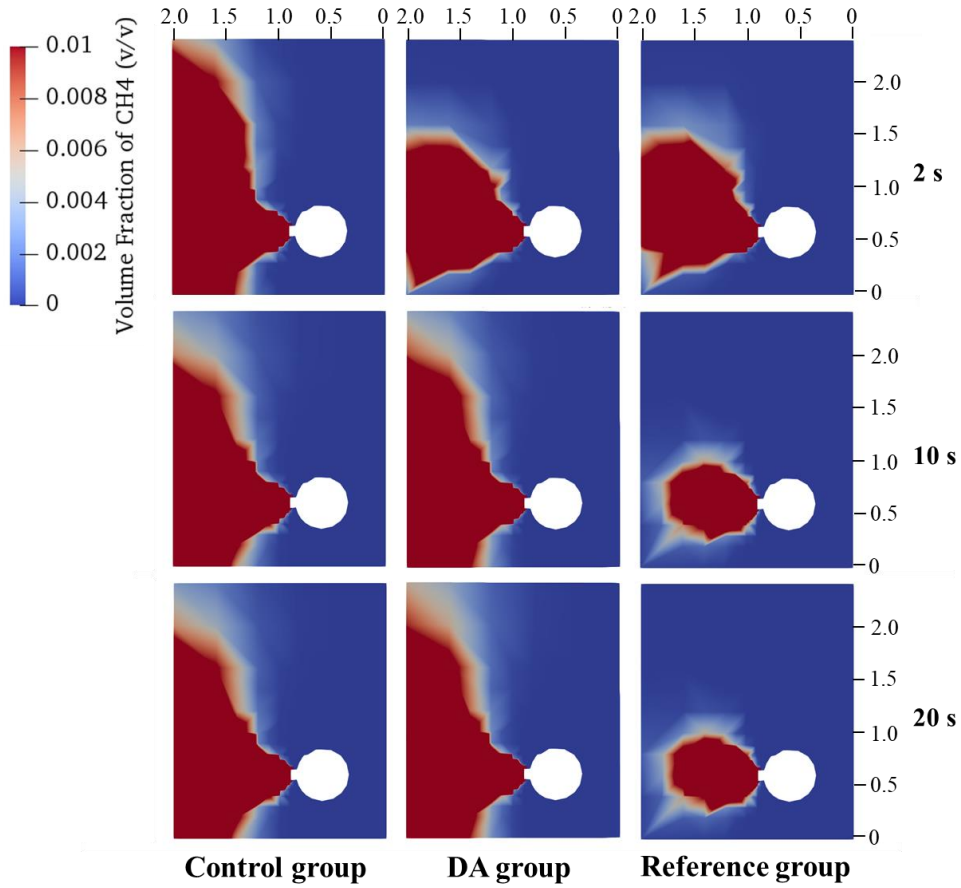


Fig. 9 Comparison between the control group, the DA group, and the reference group at X=40 m cross-section.

According to the specific layout of observation sites in Fig. 7, the above-mentioned horizontal and vertical sections ($Y=1$ m and $X=40$ m) are distributed with 28 and 12 observation sensors respectively. To evaluate the accuracy of the proposed model in handling the gas concentration correction where there is no observation sites distribution, the horizontal ($Y=0.75$ m) and vertical sections ($X=52.5$ m) are extracted for further comparison, which is shown in Fig. 10 and Fig. 11. It suggests that the gas concentration distribution of the DA group can obtain a good revision with the progress

1 of data assimilation. Therefore, the proposed model can be helpful to realize the
2
3
4 reasonable prediction of the gas concentration distribution in the whole computational
5
6
7 domain even in the section without available observation data.
8
9

10
11
12
13
14
15
16
17
18
19
20
21
22
23
24
25
26
27
28
29
30
31
32
33
34
35
36
37
38
39
40
41
42
43
44
45
46
47
48
49
50
51
52
53
54
55
56
57
58
59
60
61
62
63
64
65

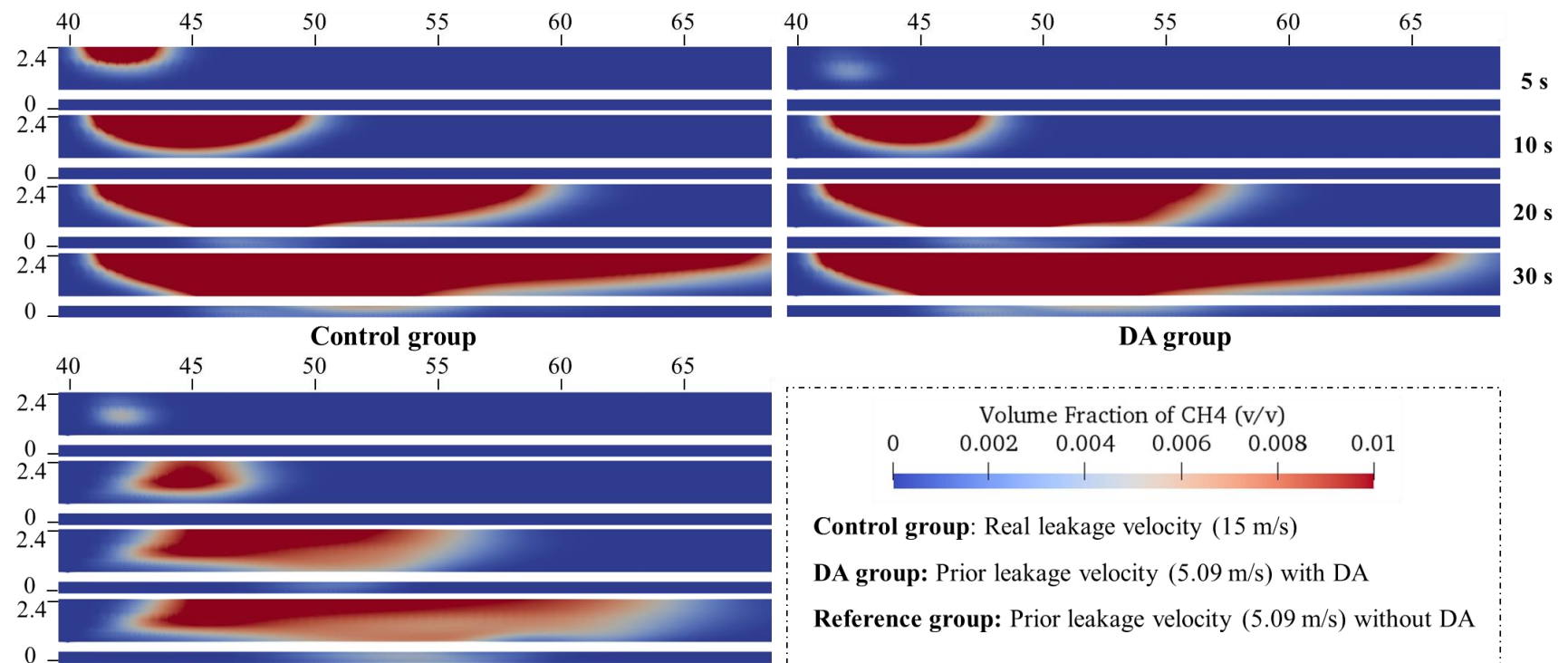


Fig. 10 Comparison between the control group, the DA group, and the reference group at Y=0.75 m cross-section.

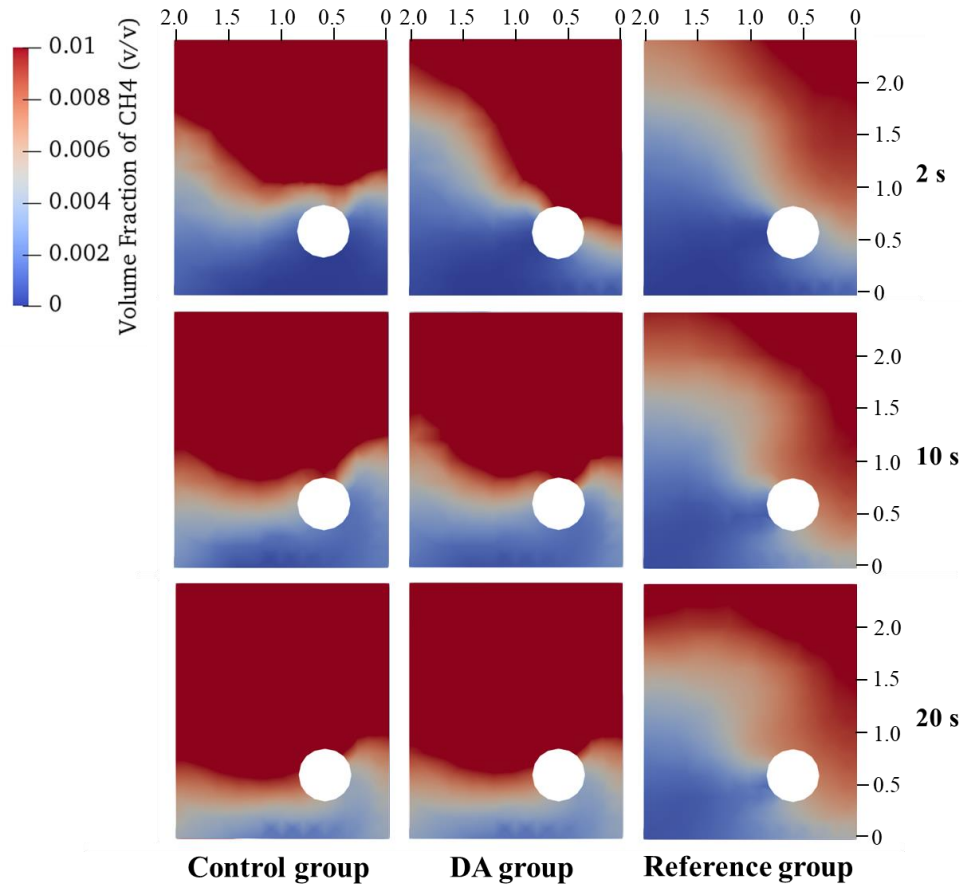


Fig. 11 Comparison between the control group, the DA group, and the reference group at X=52.5 m cross-section.

Furthermore, in order to evaluate the prediction accuracy of the proposed model quantitatively, four statistical performance measures (SPMs), i.e., the fractional bias (FB), the normalized mean square error (NMSE), the correlation coefficient (R), and the fraction of predictions within a factor of two of observations (FAC2) (Chang and Hanna, 2004), are employed for the quantitative comparison of specific gas concentration values at the observation sites. And the calculation of statistical

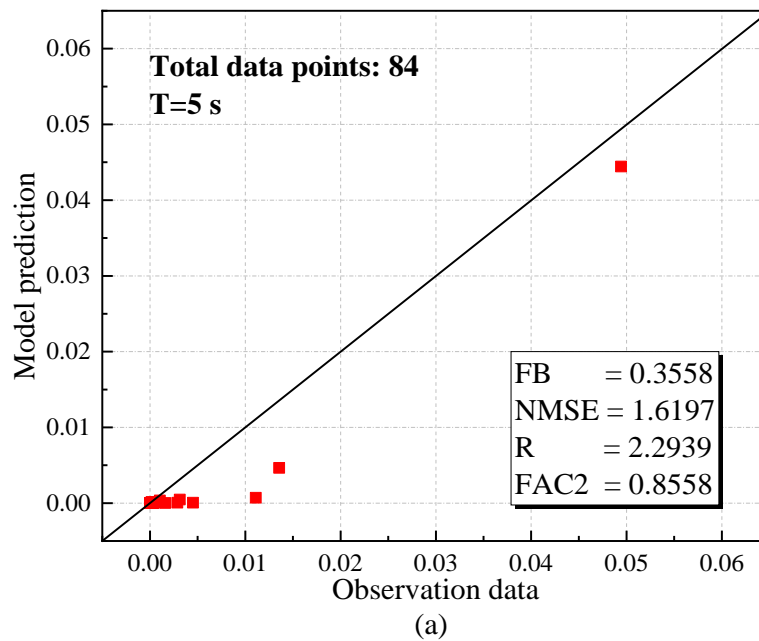
performance measures, corresponding acceptable intervals, and ideal values are detailed in Table 4 (Zhang et al., 2014; He et al., 2021). Where C_p and C_o are gas concentration values obtained from the model prediction and observation data, overbar (\bar{C}) represents the average over the dataset, σ is the standard deviation.

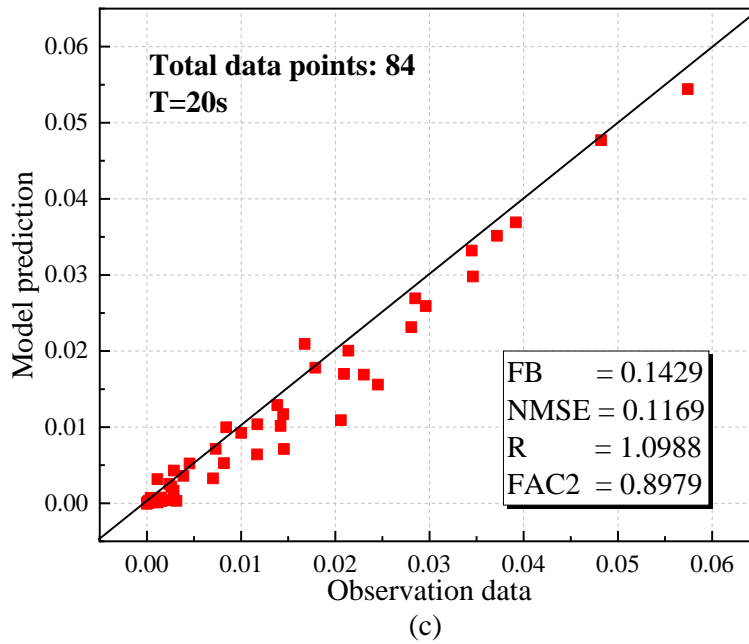
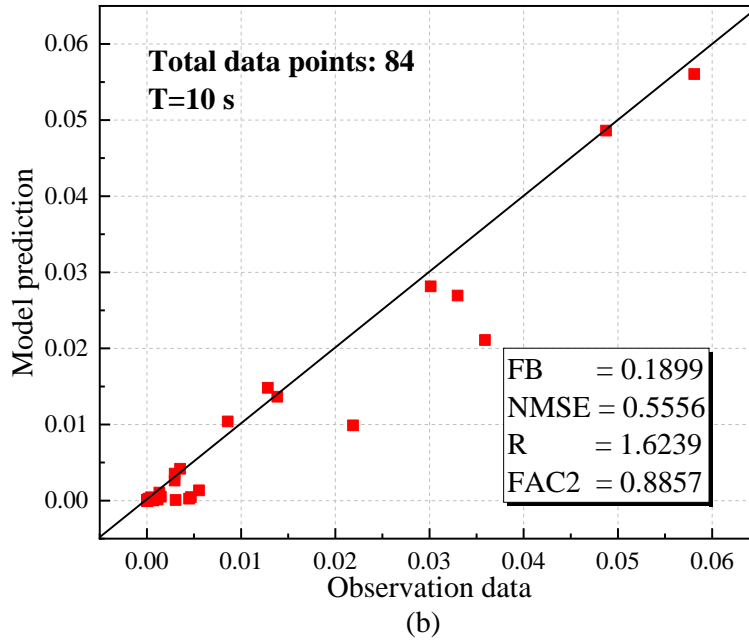
Table 4 Calculation of statistical performance measures and corresponding acceptable intervals.

Name	Formula	Acceptable intervals	Ideal value
FB	$\frac{(\bar{C}_o - \bar{C}_p)}{0.5(\bar{C}_o + \bar{C}_p)}$	$-0.3 \leq \text{FB} \leq 0.3$	0
NMSE	$\frac{((C_o - C_p)^2)}{\bar{C}_o \bar{C}_p}$	$\text{NMSE} \leq 4$	0
R	$\frac{((C_o - \bar{C}_o)(C_p - \bar{C}_p))}{\sigma_{C_p} \sigma_{C_o}}$	/	1
FAC2	$\frac{C_p}{C_o}$	$0.5 \leq \text{FAC2} \leq 2$	1

Fig. 12 presents the scatter plots of gas concentration extracted from the control group and DA group at observation sites, in which all 84 data points used for data assimilation are taken into account. There is a quite difference between observation data and the model prediction at 5 s, Almost all statistical performance measures show an unacceptable deviation compared with the corresponding ideal values except for a relatively reasonable value of FAC2. However, such a reasonable value is attributed to the poor performance of the FAC2 because little concentration information can be

1 captured by observation sensors at the initial leakage stage, i.e., there are too many zero
 2
 3
 4 values in both observation data and model prediction. Therefore, the average value
 5
 6
 7 (0.8558) of the FAC2 cannot essentially reveal the model performance at T=5 s. With
 8
 9
 10 the processing of data assimilation, the model predictions are well consistent with the
 11
 12
 13 observation data, in which all four statistical performance measures gradually approach
 14
 15
 16 the ideal values. In this study, a reasonable prediction can be achieved at T= 20 s and
 17
 18
 19 very optimistic results at T=30 s, which means the errors resulting from initial-guess
 20
 21
 22 leakage velocity, dynamic ventilation, and complex facilities, can be successfully
 23
 24
 25 suppressed by the proposed model. Therefore, the proposed model has a significant
 26
 27
 28 effect on the improvement of gas leakage and dispersion prediction.
 29
 30
 31
 32
 33





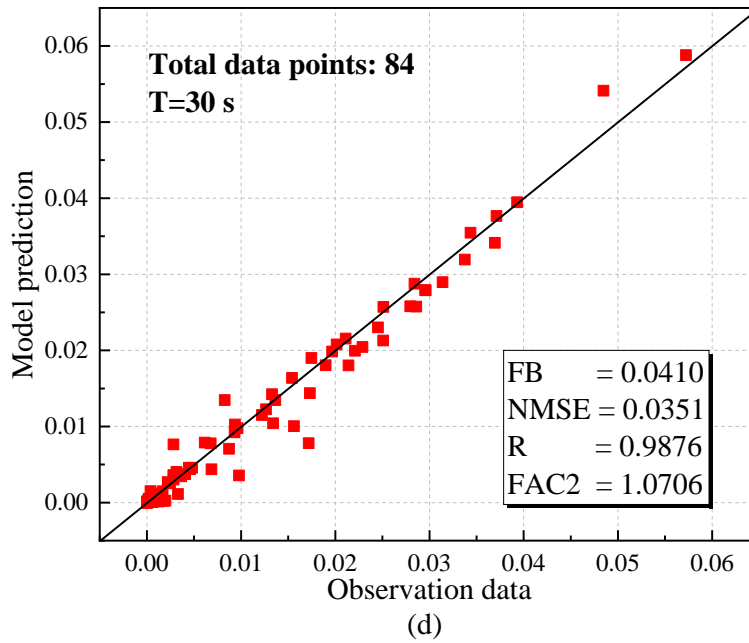
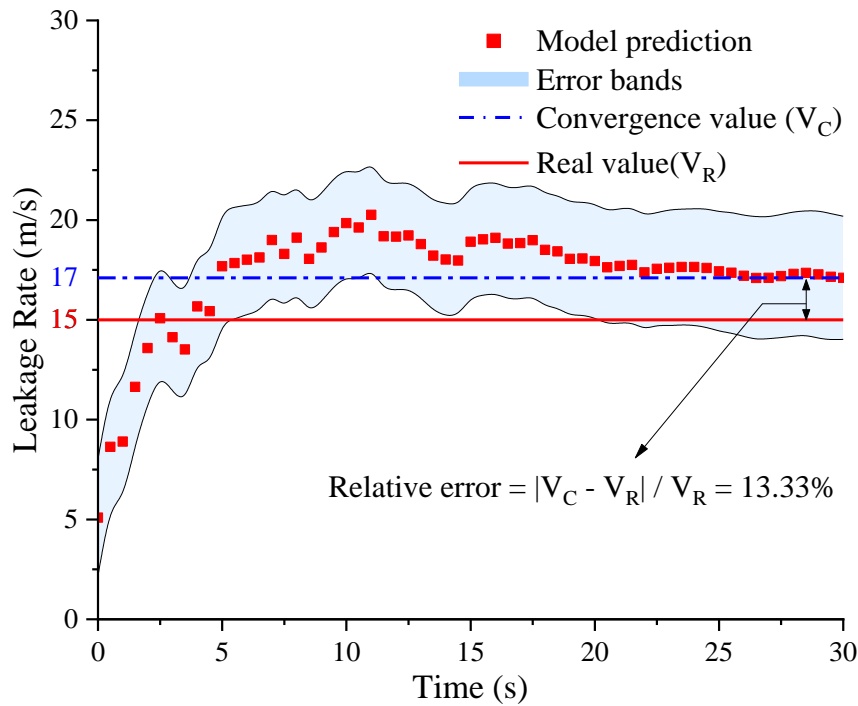


Fig. 12 Scatter plots of observation data and model prediction.

3.2.3 Estimation of gas leakage rate

Fig.13 presents the revision process of the gas leakage rate by using the proposed model and the quantitative comparison between the real leakage rate and model prediction. It can be seen that there is an apparent underestimation existing in the leakage rate with 42.67% relative errors at the initial stage of the accidental leakage. That is because the initial-guess leakage velocity can only obtain limited revision due to the lack of observation data. As a growing amount of observation data are integrated into the gas dispersion CFD model, the reconstructed leakage velocity shows a gradual trend of approaching the real value. Finally, the estimation of leakage velocity became stable at around 17 m/s after 25 s, in which the convergence results of the 3D-STE model prediction have been achieved. The max relative error between the model

1 prediction and the true value was 42.39 % at the initial stage, and the relative error of
 2
 3
 4 the model prediction approach around 13.33% from 25 s to the end due to the estimation
 5
 6
 7 of leakage velocity became stable gradually. Therefore, it can be concluded that the
 8
 9
 10 proposed 3D-STE model is an effective tool to provide a reasonable estimation of gas
 11
 12
 13 leakage velocity with high similarity to the actual leakage velocity despite huge errors
 14
 15
 16 existing in the initial-guess leakage velocity.
 17
 18
 19
 20



21
 22
 23
 24
 25
 26
 27
 28
 29
 30
 31
 32
 33
 34
 35
 36
 37
 38
 39
 40
 41
 42
 43
 44
 45
 46 Fig. 13 Revision process of the leakage rate by the 3D-STE model.
 47
 48
 49

50 **4. Application discussion** 51 52 53

54 In this section, we present an exploratory discussion with an emphasis on the
 55
 56
 57 practical application of the proposed model in actual utility tunnels. A feasible
 58
 59
 60
 61
 62
 63
 64
 65

1 framework is proposed to guide the application of this model for predicting gas leakage
2
3
4 and dispersion and supporting emergency response treatment. Meanwhile,
5
6
7 recommendations for future works are elaborated for improving the proposed model
8
9
10 and facilitating the application of the proposed model.
11
12

13 **4.1 A framework for 3D-STE model application**

14
15
16
17
18 Compared to the previous studies on the source term estimation of gas leakage
19
20
21 accidents in confined space scenarios, the proposed 3D-STE model integrated
22
23
24 advantages of the three-dimensional CFD-based model and gas sensor networks while
25
26
27 the EnKF algorithm helps to bridge the gap between simulation results and
28
29
30 measurement data. Moreover, the dynamic ventilation pattern of utility tunnels is also
31
32
33 involved. In summary, it obtains a good improvement in the following aspects:
34
35
36

37
38 (i) Except for reconstructing the leakage source, the three-dimensional
39
40
41 spatiotemporal gas concentration distribution can be obtained by the proposed model
42
43
44 because the CFD-based gas dispersion model is integrated accounting for three-
45
46
47 dimensional facilities layout, turbulent diffusion, and gravity-driven multicomponent
48
49
50 transportation. Such a precise gas concentration distribution can provide more risk-
51
52
53 related information for decision-makers such as dispersion distance and explosive area
54
55
56
57
58 of leaking gas.
59
60
61
62
63
64
65

1 (ii) The dynamic ventilation pattern based on real-time alarm concentration allows
2
3
4 a more realistic reproduction of the “two-stage” gas dispersion process dominated by
5
6
7 normal and accidental ventilation conditions respectively. It can help to reduce the
8
9
10 difference between simulation results and actual situations, which benefits a more
11
12
13 accurate consequence assessment.
14
15

16
17 Fig. 14 provides a feasible framework for the application of the 3D-STE model in
18
19
20 actual utility tunnel scenarios. Firstly, the numerical model should be built according to
21
22
23 the geometric characteristics of specific utility tunnels. In normal scenarios, i.e., no
24
25
26 leakage occurrence, the available data collected by various sensors can be used to
27
28
29 initialize the numerical model for simulating a steady flow field in advance. When an
30
31
32 unexpected leakage accident happened, some theoretical and empirical methods can be
33
34
35 employed to calculate the prior source term as possible as close to the real source term.
36
37
38 Then the 3D-STE model can predict the three-dimensional gas concentration
39
40
41 distribution and reconstruct the source term by integrating the measurement data into
42
43
44 numerical simulations. The real-time display of the prediction results can be obtained
45
46
47 as well as some risk-related information such as source term, dispersion distance, and
48
49
50 explosive area can be collected to support decision-making. Finally, the proposed 3D-
51
52
53 STE model can be integrated into the digital system of utility tunnels. A smart platform
54
55
56
57
58
59
60
61
62
63
64
65

and a data warehouse can be developed for the whole process management and data exploits of the digital system. Hence, it helps to assist safety operations of utility tunnels by furnishing control recommendations to decision-makers in accidental situations, such as manual shutdown, rush repair, and dynamic ventilation strategy.

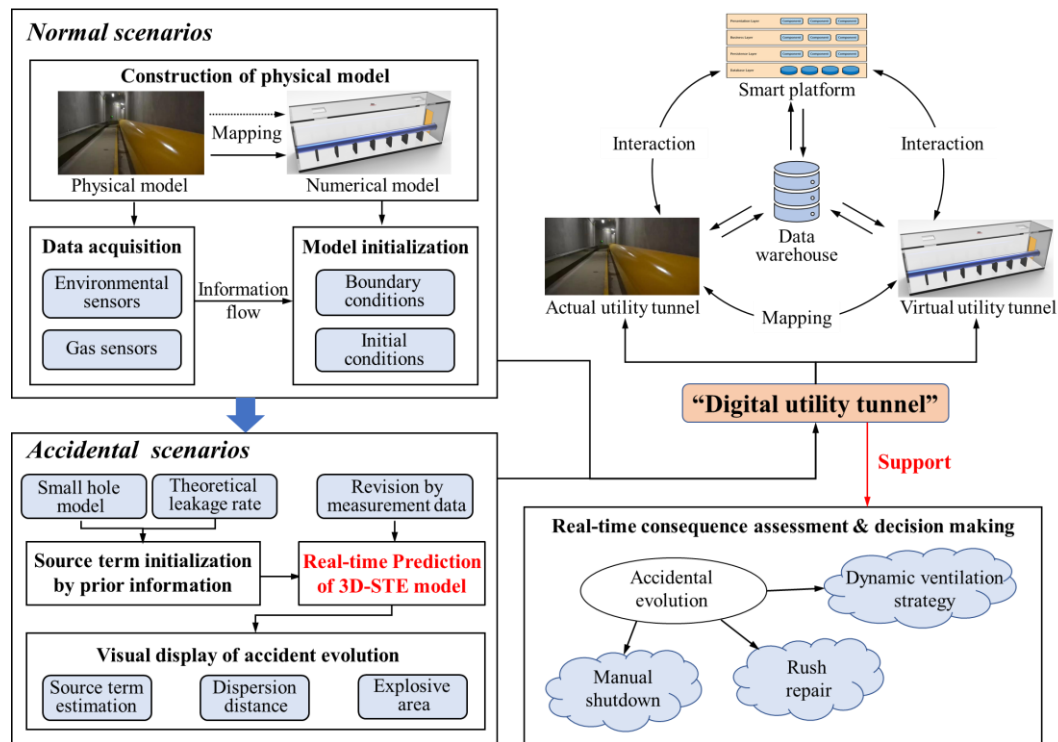


Fig. 14 Framework of the digital utility tunnel.

4.2 Recommendation for future works

(1) Timely emergency response and risk treatment are urgent needs for accidental scenarios. Graphics Processor Units (GPUs) emerged as a major paradigm for resolving complicated computational tasks, making them more appealing for the solution of massive systems. Because both the algebraic matrix solving of the CFD model and the multi-ensemble structure of the EnKF model show good parallelism, the proposed 3D-

1 STE model would achieve faster source term estimation and gas concentration
2
3
4 distribution prediction by combining GPU speed-up techniques.
5
6

7 (2) The emerging data-driven techniques have great potential to be served as the
8
9 surrogate model for either the CFD-based gas dispersion prediction model or the source
10
11 term estimation model. Given the high data volume requirements of data-driven
12
13 techniques, the developed gas dispersion model can be used to expand the data volume
14
15 and help develop a more efficient gas dispersion prediction model. As more and more
16
17 high-confidence data (e.g., experimental data and field test data) are available, the
18
19 accurate source term estimation model is possible to be developed by using data-driven
20
21 techniques.
22
23
24
25
26
27
28
29
30
31
32

33 (3) Moreover, the combination of the risk-based model can benefit the decision-
34
35 making more comprehensively. With the combination of quantitative gas concentration
36
37 distribution provided by the proposed model, the risk-based model can consider more
38
39 risk-related factors such as ignition probability and safety barriers, which provide more
40
41 comprehensive recommendations to the emergency response and risk treatment.
42
43
44
45
46
47
48
49
50

51 **5. Conclusion**

52 This study proposed a three-dimensional source term estimation (3D-STE) model
53
54
55
56 with the integration of the CFD-based gas dispersion model and ensemble Kalman filter
57
58
59
60

1 (EnKF) algorithm. It could be helpful to achieve improved three-dimensional gas
2
3
4 concentration spatiotemporal distribution prediction and leakage source estimation
5
6
7 based on available observation data.
8
9

10 The CFD-based gas dispersion model was developed based on the
11
12 *rhoReactingBuoyantFoam* embedded in the OpenFOAM platform. And it was
13
14 validated by experimental data obtained from a gas release scenario of the confined
15
16 utility tunnel system. The results demonstrated that the simulation results calculated by
17
18 the gas dispersion model are in good agreement with the experimental data. Therefore,
19
20 this model can be utilized as an effective tool to simulate the natural gas leakage and
21
22 dispersion characteristics in tunnel-related scenarios. The 3D-STE model is built based
23
24 on the validated gas dispersion model and EnKF algorithm. And the twin experiment
25
26 was designed to validate the effectiveness of the proposed model qualitatively and
27
28 quantitatively. The results showed that this proposed model is capable of addressing the
29
30 practical leakage accidents of the utility tunnel in the presence of dynamic ventilation
31
32 conditions. The revised gas concentration spatiotemporal distribution and reasonable
33
34 leakage source information can be obtained after a period of data assimilation, which
35
36 aids in timely emergency response in the event of an unexpected leakage accident.
37
38 Finally, a practical framework is elaborated and thus can provide guidance for the
39
40
41
42
43
44
45
46
47
48
49
50
51
52
53
54
55
56
57
58
59
60
61
62
63
64
65

1 application of the 3D-STE model.
2
3

4 **Acknowledgements** 5 6

7 This work was supported by the National Natural Science Foundation of China (Grant
8 No. 52174223) and the National Key Research and Development Program of China
9
10
11 (Grant No. 2017YFC0805001).
12
13
14
15
16

17 **References** 18 19 20

21 Anderson, J., 2007. An adaptive covariance inflation error correction algorithm for
22
23
24 ensemble filters. *Tellus*. 59, 210-224.
25
26

27 Bai, Y., Zhou, R., Wu, J., 2020. Hazard identification and analysis of urban utility
28
29
30 tunnels in China. *Tunnelling and Underground Space Technology*. 106, 103584.
31
32

33
34 Bu, F., Liu, Y., Wang, Z., Xu, Z., Chen, S., Hao, G., 2021. Analysis of natural gas
35
36
37 leakage diffusion characteristics and prediction of invasion distance in utility
38
39
40 tunnels. *Journal of Natural Gas Science and Engineering*. 96, 104270.
41
42
43

44 Broere, W., 2016. Urban underground space: Solving the problems of today's cities.
45
46
47 *Tunnelling and Underground Space Technology*. 55, 245-248.
48
49
50

51 Carneiro, F., Moura, L., Rocha, P., Lima, R., Ismail, K., 2019. Application and analysis
52
53
54 of the moving mesh algorithm AMI in a small scale HAWT: Validation with field
55
56
57 test's results against the frozen rotor approach. *Energy*. 171, 819-829.
58
59
60

1 Chang J., Hanna, S., 2004. Air quality model performance evaluation. *Meteorology and*
2
3
4 *atmospheric physics.* 87, 167-196.
5
6

7 Cai, J., Wu, J., Yuan, S., Liu, Z., Kong, D., 2021. Numerical analysis of multi-factors
8
9
10 effects on the leakage and gas diffusion of gas drainage pipeline in underground
11
12
13
14 coal mines. *Process Safety and Environmental Protection.* 151, 166-181.
15
16

17 CPS, 2015. *Technical Specification for Urban utility Tunnel Engineering*, GB 50838–
18
19
20
21 2015. Planning Press, China.
22
23

24 Duan, R., Liu, W., Xu, L., Huang, Y., Shen, X., Lin, C. H., Liu, J., Chen, Q., Sasanapuri,
25
26
27 B., 2015. Mesh type and number for the CFD simulations of air distribution in an
28
29
30 aircraft cabin. *Numerical Heat Transfer, Part B: Fundamentals.* 67(6), 489–506.
31
32

33
34 Fang, Z., Lin, H., Huang, H., Zheng, H., 2006. Experiment and numerical simulation
35
36
37 of gas diffusion in utility tunnels. *Engineering mechanics.* 23 (9), 189-192.
38
39

40
41 Fiates, J., Santos, R., Neto F., Francesconi, A., Simoes, V., Vianna, S., 2016. An
42
43
44 alternative CFD tool for gas dispersion CFD modelling of heavy gas. *Journal of*
45
46
47 *Loss Prevention in the Process Industries.* 44, 583-593.
48
49

50
51 He, J., Liu, L., Li, A., Ma, Y., Zhou, D., Zhou, Q., Zhan, Y., 2021. A dense gas
52
53
54 dispersion model based on revised meteorological parameters and its performance
55
56
57
58 evaluation. *Atmospheric Environment.* 344, 117953.
59
60

- 1 Ji, J., Tong, Q., Wang, L., Lin, C., Zhang, C., Gao, Z., Fang, J., 2018. Application of
2
3
4 the EnKF method for real-time forecasting of smoke movement during tunnel fires.
5
6
7 Advances in Engineering Software. 115, 398-412.
8
9
10
11 Katzfuss, M., Stroud, J., Wikle, C., 2016. Understanding the Ensemble Kalman Filter.
12
13
14 The American Statistician. 70, 350-357.
15
16
17
18 Kim, H., Park, M., Kim, C., Shin, D., 2019. Source localization for hazardous material
19
20
21 release in an outdoor chemical plant via a combination of LSTM-RNN and CFD
22
23
24 simulation. Computers and Chemical Engineering. 125, 476-489.
25
26
27
28 Kong, C., Zhang, D., Cai, R., Li, S., Zhu, R., 2020. Numerical Simulation and Analysis
29
30
31 of Diffusion Process for the Leakages of a Tunnel LNG Pipeline. Geofluids. 7, 1-9.
32
33
34
35 Lin, C., Wang, L., 2013. Forecasting simulations of indoor environment using data
36
37
38 assimilation via an ensemble kalman filter. Building and Environment. 64(6), 169-
39
40
41 176.
42
43
44
45 Li, S., Liu, X., Wang, J., Zheng, Y., Deng, S., 2019. Experimental reduced-scale study
46
47
48 on the resistance characteristics of the ventilation system of a utility tunnel under
49
50
51 different pipeline layouts. Tunnelling and Underground Space Technology. 90, 131-
52
53
54 143.-
55
56
57
58 Liu, C., Wang, D., Guo, Y., Zhang, S., He, R., 2019. Research on Diffusion Behaviors
59
60
61
62
63
64
65

1 of Leaked Natural Gas in Urban Underground Utility Tunnels. 2019 IEEE
2
3
4 International Conference on Mechatronics and Automation (ICMA). IEEE.
5

6
7
8 Lu, H., Huang, K., Fu, L., Zhang, Z., Wu, S., Lyu, Y., 2018. Study on leakage and
9
10 ventilation scheme of gas pipeline in tunnel. Journal of Natural Gas Science and
11
12 Engineering. 53, 347-358.
13
14
15

16
17
18 Mack, A., Spruijt, M., 2013. Validation of OpenFoam for heavy gas dispersion
19
20 applications. Journal of Hazardous Materials. 262, 504-516.
21
22
23

24
25 Ma, D., Zhang, X., 2016. Contaminant dispersion prediction and source estimation with
26
27 integrated Gaussian-machine learning network model for point source emission in
28
29 atmosphere. Journal of Hazardous Materials. 311, 237-245.
30
31
32

33
34
35 Ma, D., Gao, J., Zhang, Z., Zhao, H., 2021. Identifying atmospheric pollutant sources
36
37 using a machine learning dispersion model and Markov chain Monte Carlo methods.
38
39 Stochastic Environmental Research and Risk Assessment. 311, 237-245.
40
41
42

43
44
45 Marzouk, M., Othman, A., 2020. Planning utility infrastructure requirements for smart
46
47 cities using the integration between BIM and GIS. Sustainable Cities and Society.
48
49 57, 102120.
50
51
52

53
54
55 Menter, F., Kuntz, M., Langtry, R., 2003. Ten years of industrial experience with the
56
57 SST turbulence model. Proceedings of the fourth international symposium on
58
59
60

1 Turbulence. Heat and Mass Transfer, 625–632.

2
3
4 Sharma, H., Vaidya, U., Ganapathysubramanian, B., 2019. Estimating contaminant
5
6
7 distribution from finite sensor data: Perron Frobenious operator and ensemble
8
9
10 Kalman Filtering. Building and Environment. 159, 106148.

11
12
13
14 Sklavounos, S., Rigas, F., 2004. Validation of turbulence models in heavy gas
15
16
17 dispersion over obstacles. Journal of Hazardous Materials. 108, 9-20.

18
19
20
21 Tan, C., Liu, Y., Wang, T., 2017. CFD Analysis of Gas Diffusion and Ventilation
22
23
24 Protection in Municipal Pipe Tunnel. the 2017 International Conference. ACM.

25
26
27 Wang, J., Zhao, J., Lei, X., Wang, H., 2019. An effective method for point pollution
28
29
30 source identification in rivers with performance-improved ensemble kalman filter.
31
32
33 Journal of Hydrology. 577, 123991.

34
35
36
37
38 Wang, T., Tan, L., Xie, S., Ma, B., 2018. Development and applications of common
39
40
41 utility tunnels in China. Tunnelling and Underground Space Technology. 76, 92-
42
43
44 106.

45
46
47 Wang, X., Tan, Y., Zhang, T., Zhang, J., Yu, K., 2020. Diffusion process simulation and
48
49
50 ventilation strategy for small-hole natural gas leakage in utility tunnels. Tunnelling
51
52
53 and Underground Space Technology. 97, 103276.

54
55
56
57
58 Wang, Y., Huang, H., Huang, L., Ristic, B., 2017. Evaluation of Bayesian source
59
60

1 estimation methods with Prairie Grass observations and Gaussian plume model: A
2
3
4 comparison of likelihood functions and distance measures. Atmospheric
5
6
7 Environment. 152, 519-530.
8
9

10 Wu, J., Cai, J., Yuan, S., Zhang, X., Reniers, G., 2021. CFD and EnKF coupling
11
12 estimation of LNG leakage and dispersion. Safety Science. 139, 105263.
13
14
15

16
17 Wu, J., Liu, Z., Yuan, S., Cai, J., Hu, X., 2020. Source term estimation of natural gas
18
19 leakage in utility tunnel by combining CFD and Bayesian inference method. Journal
20
21 of Loss Prevention in the Process Industries. 68, 104328.
22
23
24
25

26
27 Wu, J., Yuan, S., Zhang, C., Zhang, X., 2018. Numerical estimation of gas release and
28
29 dispersion in coal mine using Ensemble Kalman Filter. Journal of Loss Prevention
30
31 in the Process Industries. 56, 57-67.
32
33
34
35

36
37
38 Xue, F., Li, X., Zhang, W., 2017. Bayesian identification of a single tracer source in an
39
40 urban-like environment using a deterministic approach. Atmospheric Environment.
41
42
43
44
45 164, 128-138.
46
47

48 Xue, F., Kikumoto, H., Li, X., Ooka, R., 2018. Bayesian source term estimation of
49
50 atmospheric releases in urban areas using LES approach. Journal of Hazardous
51
52
53
54
55 Materials. 349, 68-78.
56
57

58 Yang, C., Peng, F., Xu, K., Zheng, L., 2019. Feasibility study on the geothermal utility
59
60

1 tunnel system. *Sustainable Cities and Society*. 46, 101445.

2
3
4 Yin, X., Liu, H., Chen, Y., Wang, Y., Al-Hussein, M., 2020. A BIM-based framework
5
6
7 for operation and maintenance of utility tunnels. *Tunnelling and Underground*
8
9
10
11 *Space Technology*. 97, 103252.

12
13
14 Yuan, S., Wu, J., Zhang, X., Liu, W., 2019. EnKF-based estimation of natural gas
15
16
17 release and dispersion in an underground tunnel. *Journal of Loss Prevention in the*
18
19
20
21 *Process Industries*. 62, 103931.

22
23
24 Zhang, P., Lan, H., 2020. Effects of ventilation on leakage and diffusion law of gas
25
26
27 pipeline in utility tunnel. *Tunnelling and Underground Space Technology*. 105,
28
29
30
31 103557.

32
33
34 Zhang, X., Huang M., 2017. Ensemble-based release estimation for accidental river
35
36
37 pollution with known source position. *Journal of Hazardous Materials*. 333, 99-108.

38
39
40
41 Zhang, X., Su, G., Yuan, H., Chen, J., Huang, Q., 2014. Modified ensemble Kalman
42
43
44 filter for nuclear accident atmospheric dispersion: Prediction improved and source
45
46
47
48 estimated. *Journal of Hazardous Materials*. 280, 143–155.

49
50
51 Zhang, X., Li, Q., Su, G., Yuan, M., 2015a. Ensemble-based simultaneous emission
52
53
54 estimates and improved forecast of radioactive pollution from nuclear power plant
55
56
57
58 accidents: application to ETEX tracer experiment. *Journal of Environmental*
59
60

1 Radioactivity. 142, 78-86.
2
3

4 Zhang, X., Su, G., Chen, J., Raskob, W., Yuan, H., Huang, Q., 2015b. Iterative ensemble
5
6
7 Kalman filter for atmospheric dispersion in nuclear accidents: An application to
8
9
10 Kincaid tracer experiment. *Journal of Hazardous Materials*. 297, 329-339.
11
12

13
14 Zhang, X., Su, G., Yuan, H., Chen, J., Huang, Q., 2014. Modified ensemble Kalman
15
16
17 filter for nuclear accident atmospheric dispersion: Prediction improved and source
18
19
20 estimated. *Journal of Hazardous Materials*. 280, 143-155.
21
22

23
24 Zhou, K., Li, F., Cai, H., Yang, Y., Peng, F., Chen, L., Zhuang, J., 2021. Experimental
25
26
27 and numerical investigation of gas diffusion under an urban underground
28
29
30 construction. *Energy and Built Environment*. 2, 436-444.
31
32

33
34 Zhou, K., Li, F., Cai, H., Jing, Y., Zhuang, J., Li, M., Xing, Z., 2022. Estimation of the
35
36
37 natural gas leakage source with different monitoring sensor networks in an
38
39
40 underground utility Tunnel: From the perspectives of energy security. *Energy and*
41
42
43 *Building*. 254, 111645.
44
45
46
47
48
49
50
51
52
53
54
55
56
57
58
59
60
61
62
63
64
65